Studies in Surface Science and Catalysis 155
A. Gamba, C. Colella and S. Coluccia (Editors)

© 2005 Elsevier B.V. All rights reserved

Preparation of Zeolites via the Dry-Gel Synthesis Method

J. Weitkamp* and M. Hunger

Institute of Chemical Technology, University of Stuttgart, D-70550 Stuttgart, Germany

The principles and advantages of the dry-gel conversion (DGC) method are described for the synthesis of zeolites Beta and EU-1 with different aluminum and gallium contents in the framework. By modern analytical techniques, the processes occurring during the conversion of a dry gel into zeolite particles were investigated. In the case of the dry-gel synthesis of zeolite [Ga]Beta, XRD indicated a fast formation of the long-range order as a function of the DGC time while, as revealed by NMR spectroscopy, the rearrangement of the local structure occurs during a period of up to 65 h. This rearrangement of the local structure during the dry-gel conversion process consists of different concerted mechanisms: The dominating step at the beginning of the dry-gel conversion is a breakage of chemical bonds leading to a strong increase in the concentration of defect SiOH groups. As the DGC time increases, the number of defect SiOH groups and of Q^1, Q^2, and Q^3 silicon species decreases significantly, indicating a condensation of bonds. In the synthesis of zeolite [Ga]EU-1 it was found that the most critical parameters are the amount of water present in the autoclave during the crystallization process and the contents of sodium cations and template molecules in the dry gel.

1. INTRODUCTION

The most common method for preparing zeolites is the hydrothermal crystallization. Generally, a viscous gel consisting of an aluminum and a silicon source crystallizes at autogenous pressure at temperatures between 373 and 523 K [1]. In 1990, Xu et al. [2] introduced the vapor-phase transport (VPT) method for the synthesis of zeolite ZSM-5. In this work, the gel was prepared from aluminum sulphate, sodium silicate and sodium hydroxide. After drying in air, the gel powder was placed on a porous plate in an autoclave. At its bottom, the autoclave contained a solution of ethylenediamine and triethylamine in water. There was no contact between the dry gel and the liquid phase (see Fig. 1a). After 5 to 7 days at 453 and 473 K, the dry gel crystallized under formation of ZSM-5 particles [2]. Meanwhile, the dry-gel conversion route has also been applied for the fabrication of membranes containing, e.g., zeolites FER [3] or MOR [4] on carriers such as alumina. Often, non-volatile quaternary ammonium compounds, e.g., tetraethylammonium hydroxide or tetrapropylammonium bromide, are used as templates. Such compounds must be incorporated into the dry gel, and in these cases only water is supplied from the gas phase. The corresponding method is called steam-assisted conversion, SAC (see Fig. 1b). For both techniques (VPT and SAC), the generic term dry-gel conversion (DGC) is commonly used [5]. A variety of zeolites, e.g., ZSM-5 (MFI) [2,6], ZSM-12 (MTW) [6], Beta (*BEA) [7], EMT (EMT) [8], faujasite (FAU) [5], ZSM-22 (TON) [9], or NU-1 (RUT) [10], have been

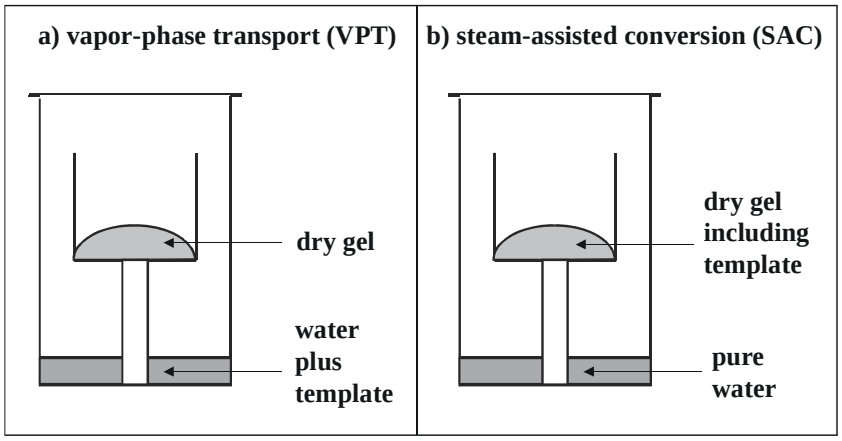

Fig. 1. Comparison of the vapor-phase transport (a) and the steam-assisted conversion method (b)

prepared via the DGC method. Bandyopadhyay et al. [11,12] applied this method for the preparation of aluminophosphate- and silicoaluminophosphate-type zeolites, such as AlPO-5 (AFI), AlPO-11 (AEL), SAPO-5 (AFI), SAPO-11 (AEL), and SAPO-34 (CHA). So far, however, only scant information is available about the chemistry of the conversion of a dry gel into a zeolite [13], while the formation of zeolitic membranes from dry gels has been investigated in more detail, mainly by using scanning electron microscopy (SEM), standard X-ray (XRD) and energy dispersive X-ray (EDX) diffraction, and pervaporation experiments [14].

The present review focuses on the conversion of dry gels into zeolites Beta (*BEA) and EU-1 (EUO) and presents some characteristic examples. The experimental techniques used for the characterization, such as SEM, XRD, and solid-state NMR spectroscopy, allowed to observe changes of the morphology, the long-range order, coordinations of framework atoms, bond connectivities, the state of the template molecules during the dry-gel conversion process, and to study the acidity of the surface sites in the obtained materials. The described synthesis routes lead to zeolites with a good crystallinity and a high concentration of Brønsted acid sites [15,16].

2. DRY-GEL SYNTHESIS OF GALLIUM-RICH ZEOLITE BETA

2.1. Preparation of zeolite [Ga]Beta by the DGC method

Zeolites [Ga]Beta were obtained, e.g., via a dry gel with an n_{Si}/n_{Ga} ratio of 8.5, which was prepared as follows: 3.0 g Cab-osil® M-5 (Fluka) were added to a suspension of the gallium source (0.58 g Ga_2O_3, Alfa Aesar) in 13.5 g of an aqueous solution of tetraethylammonium hydroxide (20 wt.-%, Acros). After stirring for 1 h, 0.95 g of a 4 N aqueous solution of NaOH followed by 5 g of water were added dropwise. The composition of the dry gel as determined by AES/ICP was: 17.01 SiO_2 : Ga_2O_3 : 0.50 Na_2O : 3.12 $(TEA)_2O$. After ageing of the gel for 2 h, it was heated in an oil bath to 353 K and dried for 4 h under stirring. Subsequently, the dry gel was ground into a fine powder, of which 1.5 g were placed in a Teflon beaker located in a stainless steel autoclave with a volume of 100 cm^3 (see Ref. [15]), which contained a small amount (0.5 g) of water at the bottom. During the crystallization, the dry gel never came into direct contact with the liquid water. The dry-gel conversion was carried out at 453 K during periods of up to 65 h. The samples obtained after quenching the dry-gel conversion at 288 K were dried in air at 353 K. To remove the template

molecules, the dried samples were calcined at 723 K in flowing nitrogen (58 l/h) with 5 vol.-% oxygen for 24 h and subsequently in air for 24 h.

The compositions of the dry gel and of the resulting zeolite [Ga]Beta were determined by AES/ICP. The morphology of the samples was investigated by SEM on a Cambridge CamScan CS44 instrument. X-ray powder diffraction patterns were recorded on a Siemens D5000 instrument using CuK_α radiation. In addition, the obtained materials were characterized by ^{1}H, ^{13}C, ^{29}Si, and ^{71}Ga NMR spectroscopy. Experimental parameters of the NMR studies are given in Ref. [15].

2.2. Long-range order of the dry-gel particles after increasing DGC times as studied by X-ray diffraction

A suitable way to study the progress of the crystallization process is to perform X-ray diffraction studies of samples taken after increasing DGC times. As an example, Fig. 2 shows the X-ray patterns of the as-synthesized materials obtained after dry-gel conversion times of 3.5, 16, 25, 50, and 65 h. The pattern obtained after 3.5 h does not show reflections at all indicating the presence of a totally amorphous material. After a conversion time of 16 h, characteristic X-ray reflections are clearly visible. A weak increase in the intensity of the main reflections at $2\theta = 8.3$ and 23.1° is observed only at elevated conversion times. However, significant changes can be observed for the weak reflections at ca. $2\theta = 16.4$ ° and $2\theta = 25$ to 31°, i.e., an intensity increase and a narrowing of the weak reflections with ongoing dry-gel conversion. This finding indicates that the long-range order is essentially established during an initial period of ca. 16 h, while thereafter only changes in the local structure occur.

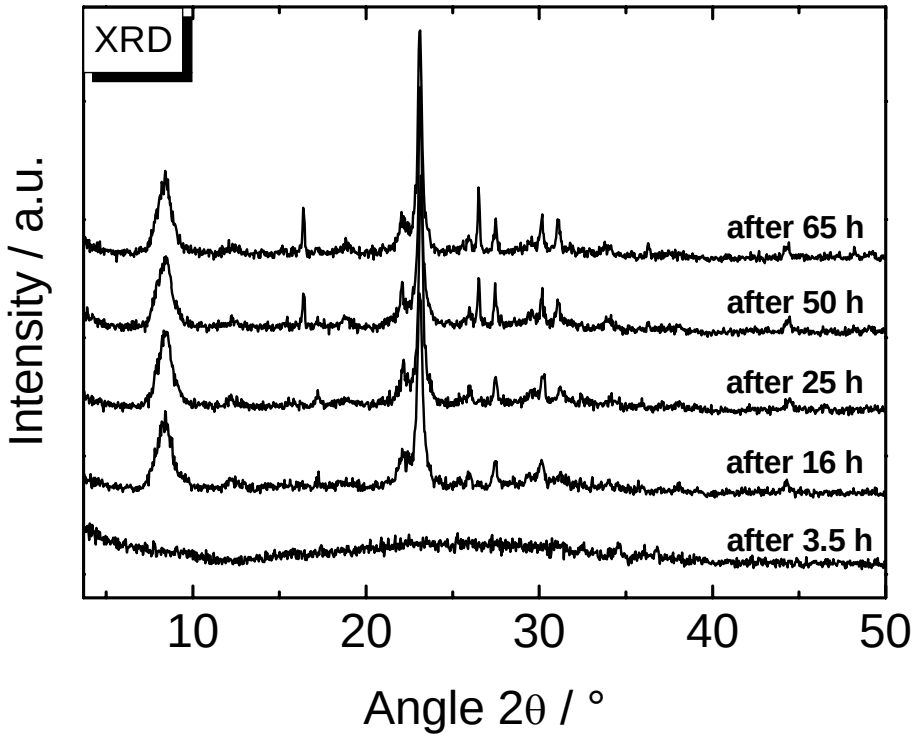

Fig. 2. X-ray patterns of as-synthesized materials obtained after DGC times of 3.5 h to 65 h [15]

The relative crystallinities of the samples obtained after different dry-gel conversion times were determined by a quantitative evaluation of the amplitude of the most intense X-ray reflection line at 2θ = 23.1°. As a reference, the amplitude of this line in the powder pattern of zeolite [Ga]Beta obtained after a conversion time of 65 h was used. This pattern (Fig. 2, top) agrees well with that of zeolite [Ga]Beta synthesized hydrothermally [17]. It has been reported that the DGC times for the synthesis of aluminum-containing zeolites Beta are significantly shorter than those for gallium-containing Beta samples, but longer for low-alumina zeolite Beta [18]. For example, Rao et al. [18] reported conversion times of 3 and 12 h for dry gels with n_{Si}/n_{Al} ratios of 15 and 365, respectively. In principle agreement with this observation, a decrease of the gallium content in the dry gel (n_{Si}/n_{Ga} = 38) led to a decrease of the crystallization rate with a relative crystallinity of only 60 % after a conversion time of 16 h, as opposed to a crystallinity of 82 % for the dry gel with n_{Si}/n_{Ga} = 8.5 after the same time [15].

2.3. Local structure of silicon atoms after increasing DGC times

By ^{29}Si MAS NMR spectroscopy of the as-synthesized materials, significant changes of the oxygen coordination of silicon atoms in the dry-gel particles as a function of the DGC time could be observed (Fig. 3). The spectrum of the fresh dry gel consists of signals at -78, -87, -97, and -107 ppm, due to Si(1OSi,3OH), Si(2OSi,2OH), Si(3OSi,1OH), and Si(4OSi) species corresponding to a Q^1, Q^2, Q^3, and Q^4 oxygen coordination, respectively [15]. With increasing DGC times, the Q^1, Q^2, and Q^3 signals strongly decrease (Fig. 3, left), and the spectra are dominated by Q^4 signals of silicon atoms with different numbers of silicon and gallium atoms in the first coordination sphere of T atoms (Fig. 3, right). The ^{29}Si MAS NMR spectrum of the sample obtained after a dry-gel conversion time of 16 h consists of signals at -114 to -111 ppm due to Si(4OSi) species (denoted Si(0Ga)) on crystallographically non-equivalent framework positions. The low-field shoulder at -101 ppm is caused by a superposition of the signals of Si(3OSi,1OGa) species (denoted Si(1Ga)) and Si(3OSi,1OH) species (denoted SiOH). The weak signal at -95 ppm is originated by Si(2OSi,2OGa) species (denoteded Si(2Ga)). The signal of Si(1Ga) species, occurring in the ^{29}Si MAS NMR spectrum of the sample obtained after a conversion time of 65 h (Fig. 3, right), is significantly narrower than in the spectra before. This finding indicates that the distribution of bond distances and bond angles in the local structure of the framework silicon atoms became smaller which is characteristic for the formation of a crystalline structure.

Considering the changes of the ^{29}Si MAS NMR spectra with increasing dry-gel conversion times, different processes can be observed. After dry-gel conversion times of up to 16 h, the intensities of the Q^1, Q^2 and Q^3 species decrease, while the signal intensity of Q^4 species increases. This indicates a healing of terminal bonds by a condensation of defect SiOH groups. After dry-gel conversion times of 16 h and more, the narrow Si(1Ga) and Si(2Ga) signals hint to an incorporation of gallium atoms at T positions into the framework of zeolite Beta.

From the relative intensities of the ^{29}Si MAS NMR signals of the final zeolite [Ga]Beta the number of gallium atoms incorporated at T positions into the zeolite framework can be calculated. In this case, the number of SiOH species contributing to the ^{29}Si MAS NMR signal at -101 ppm must be known, e.g., determined by ^{1}H MAS NMR spectroscopy of the calcined materials.

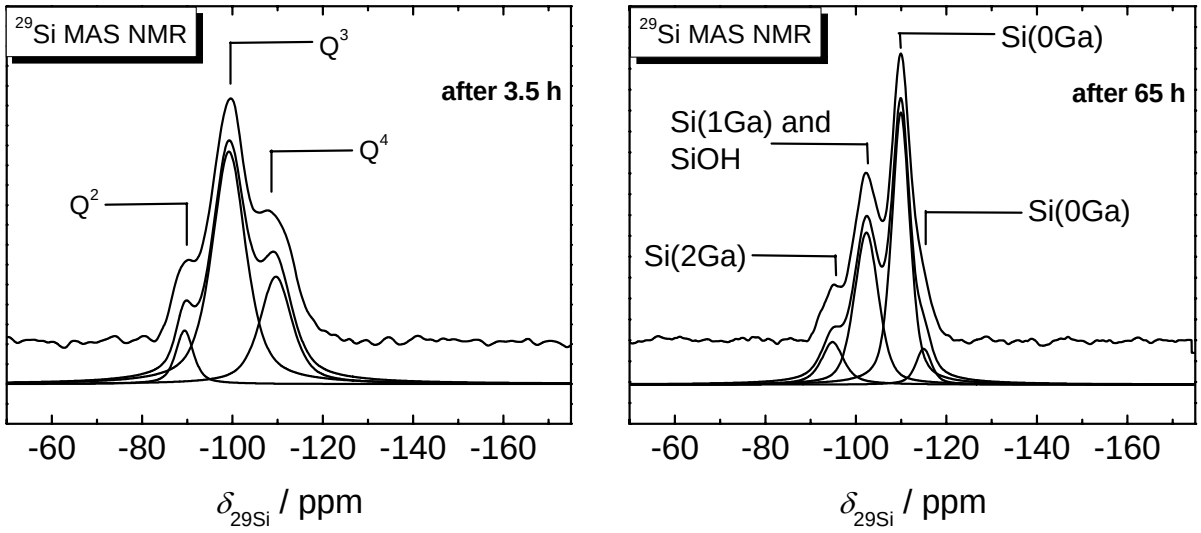

Fig. 3. ^{29}Si MAS NMR spectra of as-synthesized materials obtained after DGC times of 3.5 h (left and 65 h (right) [15]

2.4. Incorporation of gallium atoms into the zeolite framework

^{71}Ga MAS NMR spectroscopy is a useful method for investigating the local environment of gallium species in zeolite crystals. Fig. 4a shows the ^{71}Ga MAS NMR spectrum of the gallium source Ga_2O_3 consisting of signals at ca. -6 to 24 ppm and ca. 174 ppm due to hexagonal and tetrahedrally coordinated gallium species, respectively [19]. The large line width of the low-field signal is due to second-order quadrupolar line broadening and the amorphous local structure of the gallium source. In the ^{71}Ga MAS NMR spectrum of the fresh dry gel (after 0 h), significant changes can be observed: The signal of octahedrally coordinated gallium loses intensity, while the signal of tetrahedrally coordinated gallium atoms is a superposition of a broad low-field signal at ca. 174 ppm and a narrow signal at ca. 150 ppm (Fig. 4b). These findings indicate a dissolution of the gallium source during the preparation of the dry gel and the formation of first gallium tetrahedra with a higher local symmetry. In the spectra of the as-synthesized materials obtained after increasing DGC times, a systematic decrease of the signal of octahedrally coordinated gallium species at ca. 2 ppm occurs, while the intensity of the signal of tetrahedrally coordinated framework gallium species at 150 ppm increases.

After a DGC time of 65 h (Fig. 4e), the ^{71}Ga MAS NMR spectrum consists of a single signal only at 150 ppm, which indicates a complete transformation of the gallium atoms to tetrahedrally coordinated species. The ^{71}Ga MAS NMR spectra clearly show that the incorporation of gallium atoms into the zeolite framework occurs during the whole dry-gel conversion process, which was not obvious from ^{29}Si and ^{1}H MAS NMR spectroscopy. However, the strongest changes of the gallium coordination occur between DGC times of 3.5 and 16 h, where most of the Q^1, Q^2 and Q^3 silicon species disappear in the ^{29}Si MAS NMR spectra and a strong decrease of the SiOH concentration from 2.5 to 1.4 mmol/g is observed by ^{1}H MAS NMR spectroscopy. Interestingly, the conversion of the dry-gel starts with a significant increase of the number of SiOH groups, in the present case from 0.8 mmol/g (fresh dry gel) to 2.5 mmol/g (after 3.5 h), which indicates a breakage of bonds as a prerequisite for the formation of crystalline domains [15].

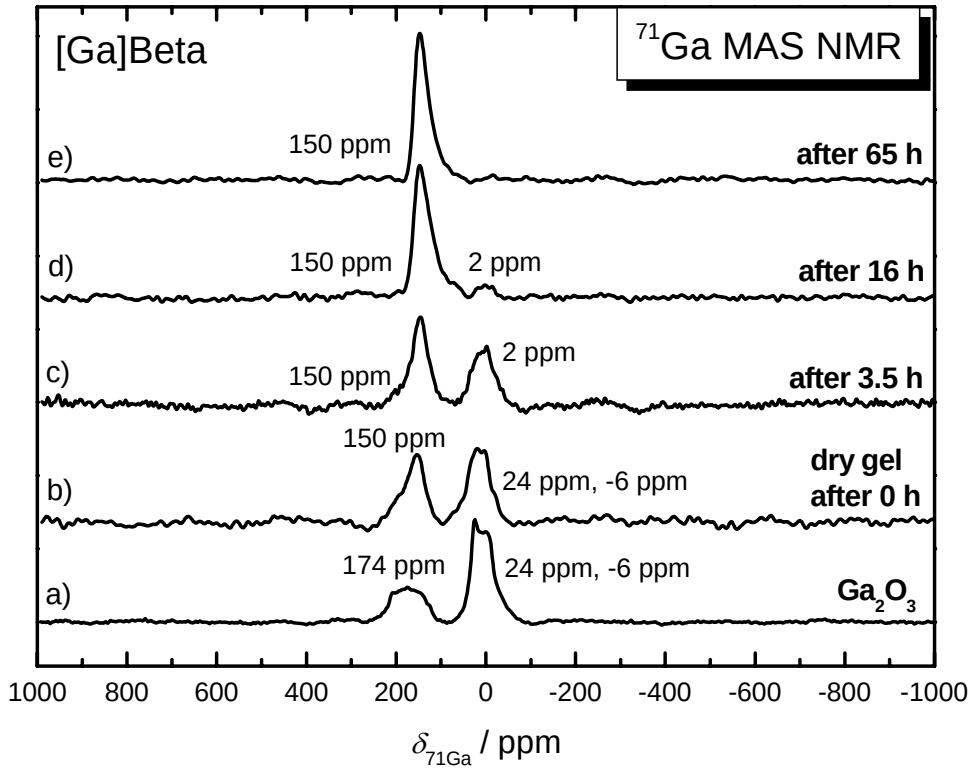

Fig. 4. ^{71}Ga MAS NMR spectra of as-synthesized materials obtained after different DGC times [15]

3. DRY-GEL SYNTHESIS OF ZEOLITE EU-1

3.1. Preparation of zeolite EU-1 by the DGC method

In a typical dry-gel synthesis of zeolite EU-1, such as a material with an n_{Si}/n_{Al} ratio of 23, a solution of 2.8 g of hexamethonium bromide (HMBr) in 30 g of water was added to 10 g of silica sol (VP AC 4038, Bayer). After stirring at room temperature for 2 h, a solution of 0.22 g sodium aluminate and 0.49 g NaOH in 3 g of water was added in the case of the preparation of zeolites [Al]EU-1. A modification of the n_{Si}/n_{Al} ratio of the dry gels was reached by changing the amount of sodium aluminate. For the adjustment of the n_{Na}/n_{Si} ratio, the amount of NaOH was varied. For the preparation of zeolites [Ga]EU-1, Ga_2O_3 was used as the gallium source. For a material with an n_{Si}/n_{Ga} ratio of 24, e.g., 0.22 g Ga_2O_3 were suspended in a solution of 0.61 g NaOH in 3 g of water. The n_{Si}/n_{Ga} ratio of the dry gels was varied by changing the amount of Ga_2O_3. For the adjustment of the n_{Na}/n_{Si} ratio, the amount of NaOH was modified (see Ref. [16]).

The resulting liquid mixtures were stirred for 2 h and dried to a powder at 353 K for 5 h under stirring. Subsequently, the dry gel was ground into a fine powder, of which 1.5 g were placed into a Teflon beaker located in a stainless steel autoclave with a volume of 100 cm^3 which contained 1.0 g water at the bottom. The dry-gel conversion was allowed to proceed at 453 K during periods of up to 7 days. The products obtained after quenching at 288 K were thoroughly washed with deionized water and dried in air at 353 K for 20 h.

To remove the template molecules, the dried samples were calcined at 813 K in flowing nitrogen with 15 vol.-% oxygen (58 l/h) for 24 h and, subsequently, in air for 24 h. The H^+-

forms of the zeolites were prepared by a fourfold ion exchange in an aqueous solution of NH_4NO_3 and subsequent thermal treatment at 723 K in vacuum ($p < 10^{-2}$ Pa) for 12 h.

3.2. Influence of the amount of template in the dry gel and the amount of water in the autoclave

The influence of the amount of template in the dry gel on the synthesis products was studied for the conversion of a dry gel with the molar composition 81.4 SiO_2 : Al_2O_3 : x Na_2O : y HMBr with x = 10.9 to 18.6 and y = 2.2 to 11.0. The results are shown in Fig. 5. According to these XRD patterns, highly crystalline zeolites [Al]EU-1 can be obtained with $n_{HMBr}/n_{Si} \geq 0.11$ and $n_{Na}/n_{Si} = 0.30$. A decrease of the template content in the dry gel (n_{HMBr}/n_{Si} = 0.09, 0.06, and 0.03) leads to the formation of α-quartz as impurity and to a loss of crystallinity. Even an increase of the sodium content in the dry gel, which favors the formation of zeolite EU-1 over zeolite EU-2 or an amorphous phase, cannot suppress the formation of α-quartz. For the synthesis of zeolite [Ga]EU-1, a similar influence of the template content on the quality of the synthesis products was observed.

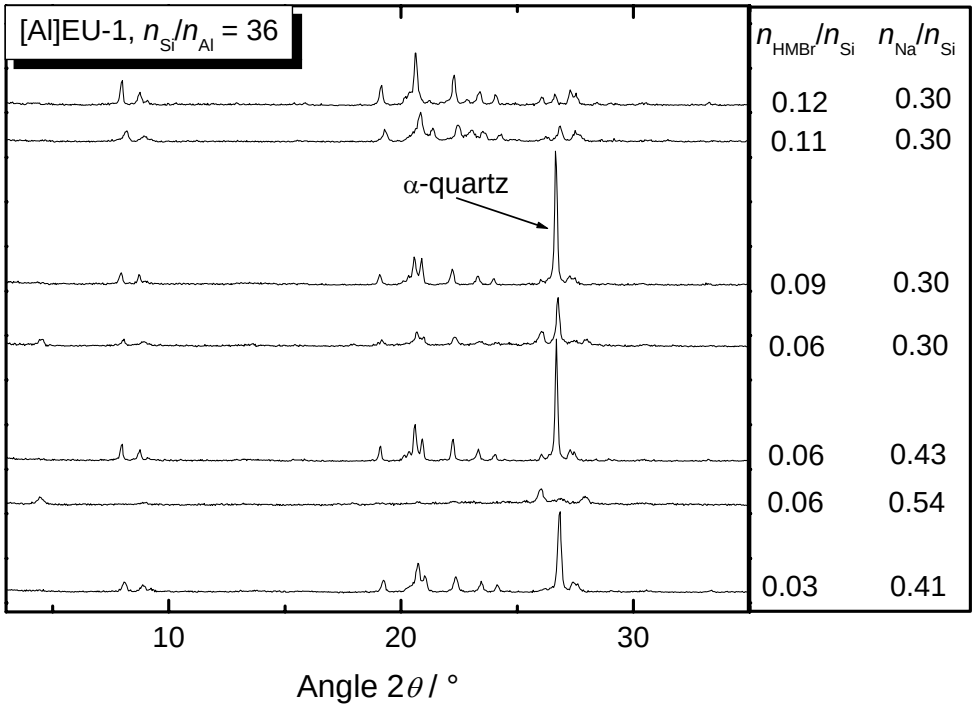

Fig. 5. X-ray patterns of as-synthesized samples obtained from a dry gel with an n_{Si}/n_{Al} ratio of 41 showing the influence of the template and sodium content on the dry-gel conversion process [16]

Fig. 6 shows the influence of the amount of liquid water in the autoclave on the conversion of a dry gel with the molar composition 61.0 SiO_2 : Al_2O_3 : 9.1 Na_2O : 7.4 HMBr. The XRD patterns clearly indicate that there is a minimum amount of water necessary for making highly crystalline zeolite EU-1. In comparison with the dry-gel synthesis of zeolite Beta, where the amount of water turned out to be a very critical factor for the crystallization process [5], zeolite EU-1 can be obtained over a large range of water contents, if $m_{H_2O}/m_{gel} \geq$

0.67 (m_{H_2O} = 1g, m_{gel} = 1.5 g). As calculated via the van der Waals equation, a mass of liquid water higher than 0.52 g in an autoclave with a volume of 100 cm^3 causes the presence of a liquid phase during the dry-gel conversion process at 453 K. This liquid water phase can be present either at the bottom of the autoclave or in the pores of the transformed solid material. Hence, the presence of liquid water is a prerequisite for the successful crystallization of zeolite EU-1 using the steam-assisted dry-gel conversion. This finding is at some variance to the dry-gel conversion process leading to zeolite Beta, where a water pressure in the range of the saturation pressure was sufficient to obtain materials with a high quality [5].

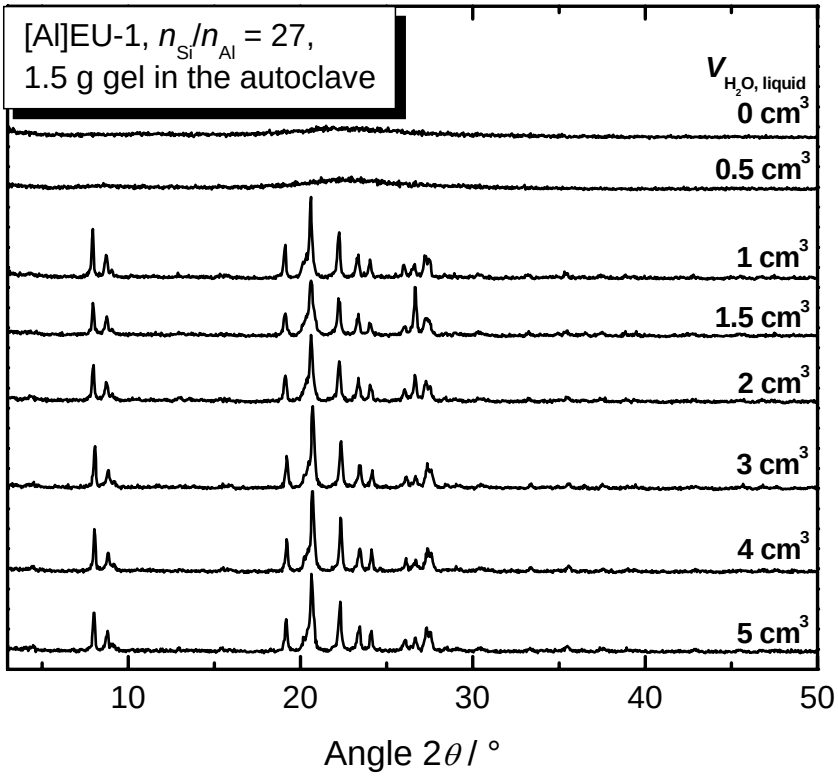

Fig. 6. X-ray patterns of as-synthesized samples obtained from a dry gel with an n_{Si}/n_{Al} ratio of 31 showing the influence of the water content on the dry-gel conversion process [16]

3.3. Synthesis and characterization of zeolites [Ga]EU-1

As shown in Table 1, the dry-gel synthesis of zeolites [Ga]EU-1 enables one to extend the range of compositions in comparison with [Ga]EU-1 materials synthesized hydrothermally towards both higher (n_{Si}/n_{Ga} < 27 [20]) and lower (n_{Si}/n_{Ga} > 50 [20]) gallium contents. As observed for the dry-gel synthesis of zeolites [Al]EU-1, the content of sodium cations in the dry gel plays an important role concerning the quality of the products. A high sodium content (n_{Na}/n_{Si} > 0.3) favors the formation of zeolites [Ga]EU-1 over an amorphous phase. In samples made from dry gels with high gallium contents ($n_{Si}/n_{Ga} \leq 34$, runs A to D), the deviations between the n_{Si}/n_{Ga} ratios of the dry gel, the as-synthesized and the H^+-forms of the zeolites are small. This finding indicates a complete conversion of the dry gel into a crystalline material without the formation of extra-framework species. In contrast, in samples made from dry gels with lower gallium contents ($n_{Si}/n_{Ga} \geq 63$, runs E and F), the n_{Si}/n_{Ga} ratios of the dry gel, the as-synthesized zeolite and its H^+-form differ significantly from each other.

This can be accounted for by extra-framework silicon species which are washed out, as also observed for aluminum-containing zeolites EU-1 [16].

The crystallinity of the as-synthesized zeolites [Ga]EU-1 was confirmed by their X-ray diffractograms: Characteristic reflections of zeolites [Ga]EU-1 [20] occurred for runs A to F, while no background reflections stemming from amorphous phases were present [16].

Table 1
n_{Si}/n_{Ga} and n_{Na}/n_{Si} ratios in the dry gels and n_{Si}/n_{Ga} ratios in the as-synthesized zeolites and in the H^+-forms of zeolites [Ga]EU-1 [16]

Run	$(n_{Si}/n_{Ga})^{dry\ gel}$	$(n_{Na}/n_{Si})^{dry\ gel}$	$(n_{Si}/n_{Ga})^{zeolite}_{a.s.}$	$(n_{Si}/n_{Ga})^{zeolite}_{H^+\text{-form}}$	Product
A	11	0.30	12	12	[Ga]EU-1
B	19	0.30	15	14	[Ga]EU-1
C	24	0.30	18	24	[Ga]EU-1
D	34	0.30	29	34	[Ga]EU-1
	63	0.30	-	-	amorphous
E	63	0.47	45	51	[Ga]EU-1
	119	0.30	-	-	amorphous
F	119	0.50	86	72	[Ga]EU-1

3.4. Characterization of the Brønsted acid sites in zeolites [Al]EU-1 and [Ga]EU-1 synthesized by the DGC method

A frequently applied technique for the quantitative determination of surface OH groups is ^{1}H MAS NMR spectroscopy of the calcined materials [21]. A typical ^{1}H MAS NMR spectrum of a dehydrated zeolite H-EU-1 consists of signals at 1.9, 2.4, and 4.0 ppm and a weak signal at 6.3 ppm, which are assigned to terminal silanol groups (SiOH), TOH groups (T: Al and Ga), bridging OH groups (SiOHT) and H-bonded SiOH groups, respectively. Generally, the bridging OH groups occurring in the ^{1}H MAS NMR spectra at 4.0 ppm are responsible for the Brønsted acidity of zeolites. The corresponding hydroxyl protons compensate the negative framework charges of tetrahedrally coordinated aluminum and gallium atoms in zeolites. In the present work, the concentration of SiOHAl and SiOHGa groups occurring at 4.0 ppm was determined by a comparison of the ^{1}H MAS NMR intensities with that of an external intensity standard.

Fig. 7 shows the concentration, c_{SiOHT}, of Brønsted acid sites plotted as a function of the concentration, c_T, of T atoms (T: Al and Ga) determined by AES/ICP. The graph shows a linear correlation between the concentration of the Brønsted acid sites and the aluminum or the gallium contents of the samples. This holds for the whole range of c_{Al} values investigated from 0.2 to 0.6 mmol/g (corresponding to n_{Si}/n_{Al} ratios of 23 and 83, see Ref. [16]) and c_{Ga} values from 0.3 to 1.1 mmol/g (corresponding to n_{Si}/n_{Ga} ratios of 12 to 72, runs A to F). The differences in the concentration of Brønsted acid sites in zeolites H-[Al]EU-1 and H-[Ga]EU-1 for the same c_T values may be due to different amounts of extra-framework aluminum and gallium species, respectively. The presence of extra-framework species in general was evidenced in Ref. [16] by ^{27}Al and ^{71}Ga MAS NMR spectroscopy. Generally, in zeolites H-[Ga]EU-1 a significant smaller number of Brønsted acidic SiOHT groups (T: Al and Ga) are formed at a given c_T value than in zeolites H-[Al]EU-1. This finding indicates, that in

dehydrated zeolites [Ga]EU-1 a smaller number of gallium atoms exist in an intact tetrahedral oxygen coordination than in dehydrated zeolites H-[Al]EU-1.

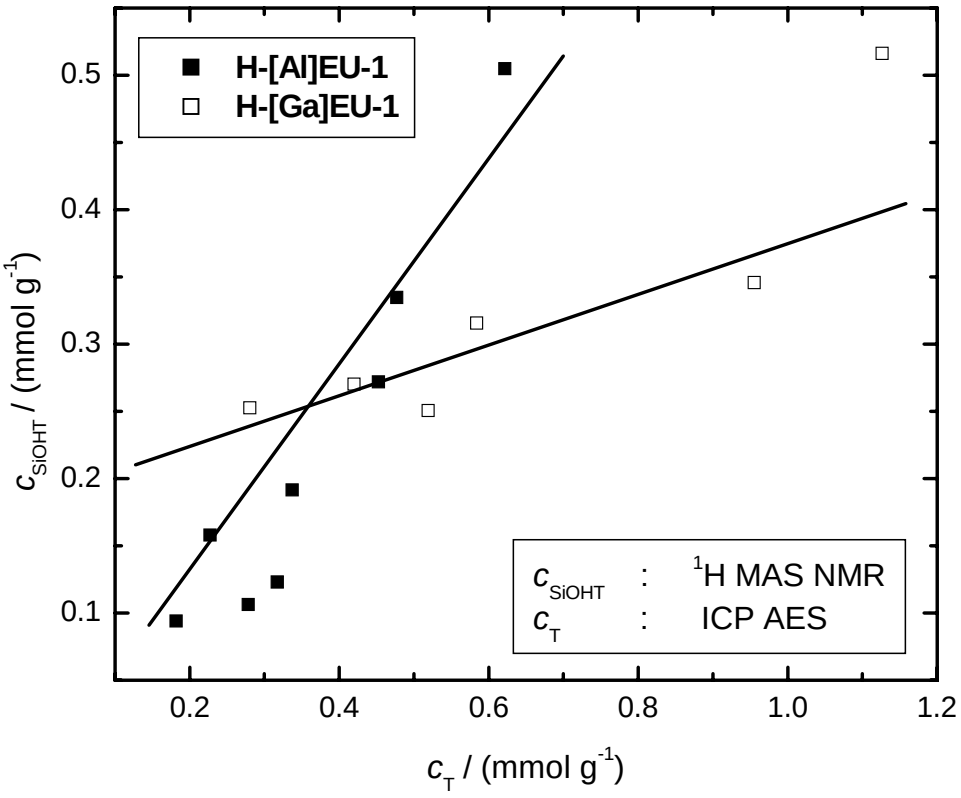

Fig. 7. Concentration of Brønsted acid sites (c_{SiOHT}), as determined by ^{1}H MAS NMR spectroscopy, plotted as a function of the concentration (c_T) of T atoms (T: Al and Ga), as obtained by AES/ICP [16]

A suitable way to study the strength of the Brønsted acidic SiOHT groups (T: Al and Ga) is the adsorption of ^{13}C-2-acetone as probe molecule and subsequent investigation of the adsorbate complexes by ^{13}C MAS NMR spectroscopy. The chemical shift of the carbonyl atoms in ^{13}C-2-acetone is sensitive with regard to an interaction of these molecules with surface sites on solid catalysts. A higher downfield shift of the ^{13}C MAS NMR signal of the carbonyl carbon atoms indicates an interaction with Brønsted sites characterized by a higher acid strength [22]. The ^{13}C MAS NMR spectra of zeolites [Al]EU-1 and [Ga]EU-1 with n_{Si}/n_{Al} and n_{Si}/n_{Ga} ratios of 23 and 24, respectively, loaded with one ^{13}C-2-acetone molecule per acid site, show signals at 214.9 and 213.3 ppm, respectively [16]. Comparing the aluminum- and the gallium-containing zeolites EU-1, therefore, the latter material has Brønsted sites with a lower acid strength. Generally, Brønsted acid sites in zeolites EU-1 have a significantly lower acid strength than those in zeolites [Ga]Beta, [Al]Beta, and [Al]ZSM-5, which cause chemical shifts of the ^{13}C MAS NMR signals of the carbonyl carbon atoms of adsorbed ^{13}C-2-acetone molecules of 219, 221, and 223 ppm, respectively.

2. CONCLUSIONS

The X-ray powder patterns of zeolites [Ga]Beta synthesized via the dry-gel conversion method and obtained after increasing conversion times show a fast formation of a long-range order during the first 16 h of the dry-gel conversion process. On the other hand, by ^{29}Si and ^{71}Ga MAS NMR spectroscopy it was evidenced that the rearrangement of the local framework structure is a more time-consuming process lasting up to 65 h.

The rearrangement of the local structure of the dry-gel particles starts with a dissolution of chemical bonds leading to a strong increase in the concentration of defect SiOH groups as indicated by ^{1}H MAS NMR spectroscopy. According to the results of ^{1}H and ^{29}Si MAS NMR spectroscopy, the further conversion of the dry gel leads to a significant diminution of defect SiOH groups and of Q^1, Q^2, and Q^3 species hinting to a condensation of Si-O-T bonds (T = Si or Ga). This silanol condensation is accompanied by the incorporation of gallium atoms into the zeolite Beta framework as evidenced by ^{71}Ga MAS NMR spectroscopy.

The dry-gel conversion method with hexamethonium bromide as template allows to prepare zeolites [Al]EU-1 and [Ga]EU-1 over a range of n_{Si}/n_{Al} ratios of 18 to 142 and n_{Si}/n_{Ga} ratios of 12 to 86, respectively. Especially for [Ga]EU-1 zeolites, the range of attainable n_{Si}/n_{Ga} ratios could be significantly extendend over the one reached previously by hydrothermal syntheses. Compared to the dry-gel synthesis of zeolite Beta, the amount of water in the autoclave plays a less important role in the case of the dry-gel synthesis of zeolite EU-1, if $m_{H_2O}/m_{gel} \geq 0.67$ is fulfilled. Critical parameters of a successful synthesis of zeolites EU-1 via the dry-gel route are the contents of sodium cations and template molecules in the dry gel. For aluminum-containing dry gels, a sodium content corresponding to an n_{Si}/n_{Al} ratio of larger than ca. 100 leads to the formation of zeolite EU-2 or to an amorphous product. The formation of α-quartz is caused by an amount of template cations in the dry gel corresponding to $n_{HMBr}/n_{Si} < 0.11$.

^{1}H MAS NMR spectroscopy of the aluminum- and gallium-containing zeolites EU-1 in the calcined H^+-form shows that a higher amount of gallium in comparison with aluminum is necessary to reach the same number of Brønsted acid sites in these materials. Their acid strength was characterized by adsorption of ^{13}C-2-acetone and subsequent investigation by ^{13}C MAS NMR spectroscopy. Due to the different electronegativities of aluminum and gallium atoms, the Brønsted acid sites in the gallium-containing zeolites H-EU-1 show a lower acid strength than those in aluminum-containing zeolites H-EU-1.

REFERENCES

[1] R. M. Barrer, Hydrothermal Chemistry of Zeolites, Academic Press, London, New York, 1982, pp. 105-182.
[2] W. Xu, J. Dong, J. Li, J. Li, F. Wu, J. Chem. Soc., Chem Commun., (1990) 755.
[3] N. Nishiyama, T. Matsufuji, K. Ueyama, M. Matsukata, Microporous Mater., 12 (1997) 293.
[4] N. Nishiyama, K. Ueyama, M. Matsukata, J. Chem. Soc., Chem. Commun., (1995) 1967.
[5] M. Matsukata, M. Ogura, T. Osaki, P.R.H.P. Rao, M. Nomura, E. Kikuchi, Top. Catal., 9 (1999) 77.
[6] R. Bandyopadhyay, Y. Kubota, N. Sugimoto, Y. Fukushima, Y. Sugi, Microporous Mesoporous Mater., 32 (1999) 81.
[7] P.R.H.P. Rao, M. Matsukata, Chem. Commun., (1996) 1441.
[8] M. Matsukata, K. Kizu, M. Ogura, E. Kikuchi, Cryst. Growth Des., 1 (2001) 509.
[9] S.G. Thoma, D.E. Trudell, F. Bonhomme, T.M. Nenoff, Microporous Mesoporous Mater., 50 (2001) 33.

[10] A. Bhaumik, T. Tatsumi, Microporous Mesoporous Mater., 34 (2000) 1.
[11] M. Bandyopadhyay, R. Bandyopadhyay, Y. Kubota, Y. Sugi, Chem. Lett., (2000) 1024.
[12] M. Bandyopadhyay, R. Bandyopadhyay, S. Tawada, Y. Kubota, Y. Sugi, Appl. Catal. A : General, 225 (2002) 51.
[13] M. Matsukata, T. Osaki, M. Ogura, E. Kikuchi, Microporous Mesoporous Mater., 56 (2002) 1.
[14] T. Matsufuji, N. Nishiyama, K. Ueyama, M. Matsukata, Microporous Mesoporous Mater., 32 (1999) 159.
[15] A. Arnold, S. Steuernagel, M. Hunger, J. Weitkamp, Microporous Mesoporous Mater., 62 (2003) 97.
[16] A. Arnold, M. Hunger, J. Weitkamp, Microporous Mesoporous Mater., 67 (2004) 205.
[17] M.L. Occelli, H. Eckert, A. Wölker, A. Auroux, Microporous Mesoporous Mater., 30 (1999) 219.
[18] P.R.H.P. Rao, K. Ueyama, M. Matsukata, Appl. Catal. A: General, 166 (1998) 97.
[19] H.K.C. Timken, E. Oldfield, J. Am. Chem. Soc., 109 (1987) 7669.
[20] G.N. Rao, V.P. Shiralkar, A.N. Kotasthane, P. Ratnasamy, in: M.L. Occelli, H.E. Robson (Eds.), Synthesis of Microporous Materials, Vol. 1, Molecular Sieves, Van Nostrand Reinhold, New York, 1992, pp. 153-166.
[21] M. Hunger, Catal. Rev.-Sci. Eng., 39 (1997) 345.
[22] G.T. Kokotailo, D. White, J. Catal., 148 (1994) 779.